A PRELIMINARY CHARACTERIZATION OF THE SPATIAL VARIABILITY OF PRECIPITATION AT YUCCA MOUNTAIN, NEVADA

Joseph A. Hevesi
U.S. Geological Survey
P.O. Box 327, M/S 721
Mercury, Nevada 89023
(702) 295-5998

Dale S. Ambos
Foothill Eng. Consultants
P.O. Box 327, M/S 721
Mercury, Nevada 89023
(702) 295-5826

Alan L. Flint
U.S. Geological Survey
P.O. Box 327, M/S 721
Mercury, Nevada 89023
(702) 295-5805

ABSTRACT

Isohyetal maps of precipitation and numerical models for simulating precipitation are needed to help characterize natural infiltration at Yucca Mountain, Nevada. A geostatistical analysis of measured precipitation was conducted to determine the spatial variability of precipitation accumulated from storm periods. Precipitation was measured during a 3.8 year period from January, 1990 to October, 1993 using a network of precipitation gages. A total of 34 winter-type storms and 12 summer-type storm, categorized using synoptic weather records, were analyzed using the 1st and 2nd statistical moments and sample variograms. Average standardized variograms indicated good spatial correlation for both storm types with only slight differences in the general spatial structure. Coefficients of variation and average relative variograms indicated that summer storms are characterized by greater variability as compared to winter storms. Models were fitted to the average summer and winter standardized variograms and compared to the sample variograms for each storm using the mean storm depth and the coefficient of variation as scaling parameters. Isohyetal maps of 4 representative storms were created using the standardized models. Results indicate that standardized models can be used to simulate the spatial distribution of precipitation depth, provided that the 1st and 2nd moments are known or can be estimated, and that identifiable deterministic trends can be included in the models. A single, fixed model representing the spatial variability of precipitation at Yucca Mountain is not recommended.

INTRODUCTION

Yucca Mountain is located approximately 100 miles northwest of Las Vegas, Nevada, in the Mojave Desert region of the Great Basin physiographic province, and is being evaluated as a potential site for a geologic repository of high-level radioactive waste[1]. Average annual precipitation at this arid site is estimated to be 6.7 inches[2]. Precipitation is a source of natural shallow infiltration and a potential source of deeper percolation through the unsaturated zone which includes the potential repository horizon[3]. Precipitation is also the source of intermittent surface runoff at Yucca Mountain, which can increase the potential for deep infiltration. A characterization of precipitation is needed to help provide input for site-scale hydrologic flow models[4].

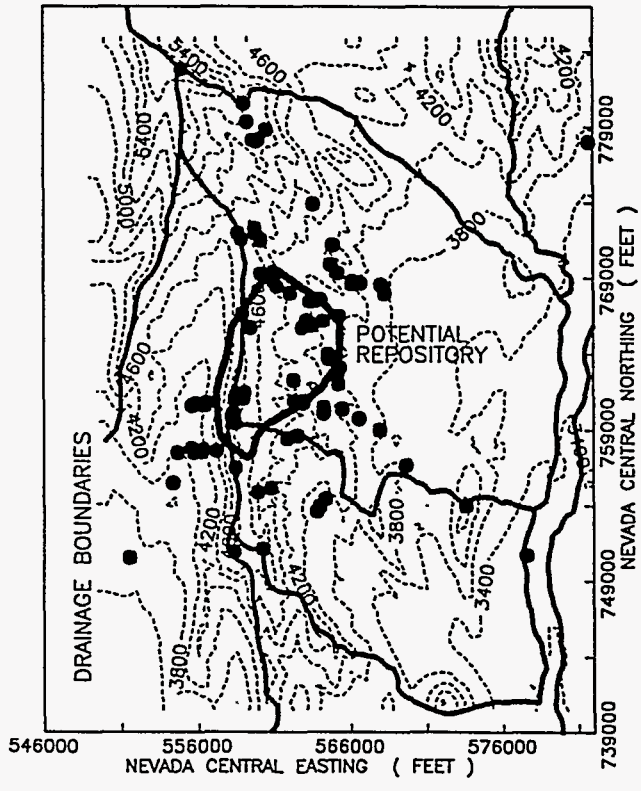

Figure 1. Map indicating non-recording precipitation gages on Yucca Mountain, surface topography, major surface drainage boundaries, and the potential repository boundary. Elevation contour interval is 200 feet.

Synoptic-scale differences between winter and summer precipitation in Southern Nevada has been documented[5]. Yucca Mountain is located along the western edge of a climatological transition zone caused by both topographical and geographical features which influence the genesis of storms relative to moisture sources[6,7]. West of the transition zone the predominant source of moisture is the Pacific Ocean and storms tend to occur during the winter season. Winter storms are stratified, occur on a regional scale, and are frontal in nature. East of the transition zone, the predominant moisture source is both the Gulf of Mexico to the southeast and the Pacific Ocean to the southwest, and storms usually occur during the southwest summer monsoon from July through August. In contrast to winter storms, summer storms tend to be localized, convective-type events that are often isolated, are usually associated with lightning, and result in brief but occasionally heavy precipitation. Although most precipitation at Yucca Mountain occurs during the winter season, sporadic summer season precipitation does occur as a result of the southwest monsoon[8,9]. Convective type storms can also occur during the spring or fall, but tend to be associated with cold upper-level lows passing over the region with the Pacific Ocean as the moisture source.

The objective of this study was to characterize the spatial variability of precipitation within the domain of the natural catchments overlying the potential repository, and to define preliminary geostatistical models based on differences in storm type for the numerical simulation of precipitation. Geostatistics is a technique often used to analyze and model the spatial variability of a regionalized variable[10]. Spatial variability can be defined using the variogram:

$$\gamma(h) = \frac{1}{2} E\left[(Z(x+h) - Z(x))^2\right] \qquad (1)$$

where E is the expectation operator, Z is a regionalized variable, and $(x + h)$ and (x) refer to positions within the domain of Z separated by vector h. The variogram $\gamma(h)$ defines the expected variance between a pair of "realizations", or values, of the regionalized variable as a function of the separation, or lag vector, between the two values. The variogram can be estimated by obtaining a sample, z, of the regionalized variable, and calculating the sample variogram $\gamma^*(h)$:

$$\gamma^*(h) = \frac{1}{2n} \sum_{i=1}^{n} \left[(z(x_i+h) - z(x_i))^2\right] \qquad (2)$$

where n is the number of data pairs separated by lag h for which values of the regionalized variable are known. The sample variogram is considered to be representative of the regionalized variable for n values of approximately 30 or greater and for lag values less than 1/2 the maximum lag value obtained for a given data set[10,11]. For irregularly distributed data, an average lag can be calculated for a range of values in order to obtain a sufficient number of pairs[12]. Numerical models can be fitted to the sample variogram for the purpose of estimating values of the regionalized variable between measured locations or for simulating unique realizations of the regionalized variable[10,13].

METHODOLOGY

Data Collection

An initial network of 49 non-recording precipitation gages was installed at Yucca Mountain in January, 1990[14]. The network was expanded during a 3.8 year period ending in October, 1993 to include a total of 133 gages at 108 locations (Figure 1). A listing of the Nevada Central state plane coordinates and site elevations for the non-recording gage network is provided by Ambos and Flint[14]. Most of the locations coincide with boreholes used for geophysical monitoring of natural infiltration to provide a record of precipitation for water balance studies at these sites[3]. Additional gages are located where the spatial coverage of boreholes is sparse relative to the area of interest. Three different types of gages are included in the network; the 1st type is wedge-shaped with a rectangular 2 inch by 2.5 inch orifice, the 2nd type is a circular 4 inch diameter canister, and the 3rd type is the standard National Weather Service 8 inch diameter metal gage. Measurements of precipitation depth were obtained by observing a fluid level relative to a calibration mark. Measurement resolution varied from 0.01 inches to 0.05 inches. At selected locations multiple gage types were installed. The non-recording gages supplement a network of 13 recording 8-inch tipping bucket gages (including heated gages), and are used only to provide a measure of the spatial distribution of precipitation[5].

Storm Type Identification

Storms were identified subjectively and defined as periods of measurable accumulations of precipitation bounded by dry periods lasting a minimum of 12 hours. Each storm was categorized as either winter-season frontal or summer-season convective based on storm timing and information indicating synoptic-scale storm genesis and trajectory[5]. Synoptic-scale storm movement was derived from a continuous record of geostationary weather satellite images and from daily surface and upper level weather charts for the Pacific Ocean and Western Hemisphere. A continuous chronological record of cloud to ground lightning strike location and intensity added information on convective storm development and movement within the Southern Nevada region. A time-lapse video recording of weather directly over Yucca Mountain (viewed from a horizontal distance of 12 miles) provided site-scale information on storm genesis and

movement.

Statistical Analysis

Winter and summer storms were compared using descriptive statistics for measured precipitation depth that included the coefficient of variation and the correlation coefficient of precipitation depth with gage elevation. A geostatistical analysis was conducted for all storms having a mean depth of at least 0.10 inches and consisting of at least 30 locations where precipitation was measured. This requirement was necessary for obtaining a dataset sufficient for geostatistical analysis[10,11]. Following the methodology presented by Cooper et al[12], 2-dimensional isotropic variograms were calculated using the horizontal distance separating gage locations. Weighted-average variograms were used to analyze and compare the general spatial variability of the two storm types. It was hypothesized that precipitation would have a proportional effect (a type of non-stationarity) in the time domain. To eliminate the proportional effect, an average relative variogram $\gamma^R(h)$ was calculated using:

$$\gamma^R(h) = \frac{1}{N}\sum_{i=1}^{k}\frac{n_i\gamma_i^*(h)}{m_i^2} \qquad (3)$$

where k is the number of storms, n is the number of data pairs used for calculating the variogram $\gamma^*(h)$ for storm i, m is the mean precipitation depth for storm i, and N is the sum of the data pairs for all storms. Equation 3 assumes stationarity for each storm event within the sample domain[13].

The relative variogram may be a good indicator of the average magnitude of spatial variability relative to the mean precipitation depth, but it may not be the best representation of the average spatial structure because of a possible bias caused by storms having different coefficients of variation. For a more accurate indication of the average spatial structure, an average standardized variogram $\gamma^S(h)$ was calculated using :

$$\gamma^S(h) = \frac{1}{N}\sum_{i=1}^{k}\frac{n_i\gamma_i^*(h)}{V_i} \qquad (4)$$

where V is the sample variance of precipitation depth for storm i. The average standardized variogram was used for a comparison of the spatial correlation of winter and summer storms in terms of the nugget structure, the transition structure, and the range of spatial correlation. Models fitted to the average standardized variogram were considered to be the most accurate representation of the average spatial structure. Standardized models were used to create isohyetal maps of selected storms by including the 1st and 2nd moments of storm depth as scaling parameters.

RESULTS

Description of Recorded Storms

A total of 34 winter type and 12 summer type storms measured during the study period were categorized and selected for geostatistical analysis (Table 1). The selected storms do not represent a complete record of precipitation at Yucca Mountain; approximately 30% of the storms measured were insufficient in terms of accumulated precipitation for a geostatistical analysis. Although the omitted storms are important in studying the temporal probability distribution of precipitation at Yucca Mountain, they do not contribute significantly to total precipitation.

Identified winter storms were found to be associated with the presence of an upper level trough and a surface front which often developed a low pressure center as the systems carried moisture from the Pacific Ocean eastward over the Sierra Nevada Mountains. Winter storms often included precipitation occurring as snow, especially for the higher elevations. In contrast, the general weather pattern during summer monsoon storms was an upper level high pressure ridge advancing into the southwestern United States and bringing moisture northwest from the Gulf of Mexico and northeast from the Pacific Ocean. Several late September convective-type storms were also identified as summer storms, but these were associated with cold upper level low pressure systems.

Statistical Comparison

Measured precipitation from winter season frontal-type storms for the study period exceeded summer season convective-type storms in terms of total precipitation, mean storm depth, maximum storm depth, storm duration, and storm frequency (Table 1). Identified storm periods included a maximum of 4 separate events for winter storms and 2 separate events for summer storms. Annual precipitation was variable; 1990 was a relatively dry year, while 1992 and the partial year of 1993 were relatively wet due to a high frequency of winter season storms. The maximum mean storm depth and the maximum-maximum storm depth were both measured following the winter storm of December 7, 1992. The greatest frequency of convective storms occurred during the summer season of 1991. The maximum mean storm depth for a convective storm was measured for the storm ending on September 4, 1991. The total record was considered representative of the expected pattern of wet winter seasons and more sporadic summer season precipitation at Yucca Mountain.

A comparison of the standard deviation of storm depth with mean storm depth indicated a trend of increasing variability with increasing mean storm depth for both storm types, with summer storms having the

Year	Starting Date Month/Day	Ending Date Month/Day	Storm Type	Number of Events	Total Time (hours)	Number of Data	Mean Precip. (inches)	Max. Precip. (inches)	Min. Precip. (inches)	St. Dev. Precip. (inches)	Coeff. of Var.	Elev. Corr. Coeff.
90	01 / 17	01 / 17	Winter	1	8.0	49	0.28	0.51	0.08	0.094	0.34	-0.39
90	04 / 20	04 / 20	Winter	1	2.2	79	0.22	0.31	0.10	0.036	0.17	0.26
90	05 / 28	05 / 28	Winter	1	17.9	84	0.44	0.66	0.10	0.076	0.17	0.23
90	07 / 14	07 / 16	Summer	2	5.7	84	0.53	1.75	0.08	0.319	0.60	-0.06
90	08 / 15	08 / 15	Summer	1	1.2	80	0.37	0.92	0.04	0.197	0.53	0.17
90	09 / 23	09 / 23	Summer	1	4.5	71	0.38	0.93	0.15	0.137	0.36	-0.45
90	11 / 19	11 / 20	Winter	1	13.2	93	0.12	0.21	0.04	0.036	0.31	0.12
91	02 / 27	02 / 28	Winter	1	23.0	87	0.67	0.97	0.43	0.088	0.13	-0.56
91	03 / 01	03 / 01	Winter	1	9.5	84	0.43	0.63	0.06	0.100	0.23	0.50
91	03 / 19	03 / 19	Winter	1	8.0	92	0.36	0.56	0.10	0.098	0.27	-0.40
91	03 / 20	03 / 21	Winter	1	11.7	91	0.63	0.99	0.15	0.203	0.32	-0.63
91	03 / 27	03 / 27	Winter	1	13.1	90	0.64	1.10	0.17	0.225	0.35	-0.76
91	05 / 01	05 / 01	Winter	1	22.9	80	0.32	0.45	0.09	0.090	0.28	-0.11
91	08 / 01	08 / 01	Summer	1	0.6	80	0.30	0.88	0.01	0.192	0.64	-0.04
91	08 / 10	08 / 11	Summer	1	0.2	52	0.13	0.36	0.01	0.103	0.80	0.20
91	08 / 12	08 / 12	Summer	1	3.9	92	0.41	0.97	0.13	0.123	0.30	-0.11
91	08 / 31	09 / 04	Summer	2	13.3	89	0.89	1.95	0.12	0.428	0.48	0.29
91	09 / 28	09 / 28	Summer	1	10.7	78	0.14	0.29	0.01	0.052	0.36	0.48
91	12 / 07	12 / 08	Winter	1	2.7	92	0.13	0.21	0.08	0.021	0.15	0.59
91	12 / 28	12 / 30	Winter	1	14.2	67	0.48	0.63	0.25	0.079	0.16	-0.50
92	01 / 03	01 / 06	Winter	4	23.2	72	1.16	1.40	0.74	0.162	0.14	-0.43
92	02 / 05	02 / 06	Winter	1	3.9	91	1.23	1.61	0.68	0.154	0.13	0.24
92	02 / 09	02 / 13	Winter	4	25.7	90	1.56	2.02	1.20	0.170	0.11	0.00
92	02 / 15	02 / 18	Winter	1	7.5	73	0.43	0.70	0.03	0.115	0.27	0.17
92	03 / 02	03 / 03	Winter	1	27.3	85	0.98	1.33	0.37	0.190	0.19	0.44
92	03 / 06	03 / 08	Winter	3	15.8	95	0.20	0.65	0.14	0.069	0.35	-0.28
92	03 / 20	03 / 23	Winter	4	17.2	95	0.64	1.13	0.22	0.146	0.23	0.08
92	03 / 27	03 / 27	Winter	1	4.7	94	1.07	1.49	0.73	0.138	0.13	0.28
92	07 / 31	07 / 31	Summer	1	0.5	53	0.14	0.51	0.01	0.148	1.09	-0.42
92	08 / 11	08 / 11	Summer	1	0.5	76	0.27	0.75	0.01	0.189	0.70	0.13
92	10 / 24	10 / 24	Winter	1	5.8	104	0.24	0.46	0.05	0.095	0.39	-0.06
92	10 / 28	10 / 30	Winter	4	17.2	103	0.27	0.48	0.08	0.068	0.25	0.51
92	12 / 07	12 / 07	Winter	1	19.5	103	2.02	2.80	0.73	0.480	0.24	-0.69
92	12 / 27	12 / 28	Winter	1	8.0	31	0.30	0.46	0.13	0.065	0.21	-0.33
93	01 / 03	01 / 06	Winter	1	M	66	0.48	0.65	0.12	0.113	0.24	-0.43
93	01 / 10	01 / 14	Winter	4	35.2	74	0.89	1.08	0.36	0.149	0.17	-0.58
93	01 / 15	01 / 18	Winter	4	17.3	76	1.40	2.05	0.89	0.223	0.16	-0.51
93	01 / 30	01 / 30	Winter	1	1.7	53	0.15	0.25	0.05	0.053	0.36	-0.08
93	02 / 07	02 / 09	Winter	3	46.4	58	1.47	1.75	0.56	0.175	0.12	-0.03
93	02 / 18	02 / 23	Winter	2	22.1	91	0.80	1.18	0.56	0.092	0.11	-0.55
93	02 / 26	02 / 28	Winter	2	9.0	91	0.80	1.05	0.28	0.200	0.25	-0.65
93	03 / 26	03 / 28	Winter	3	24.5	106	0.90	1.17	0.67	0.098	0.11	-0.10
93	06 / 05	06 / 05	Winter	1	5.8	100	0.65	0.96	0.49	0.106	0.16	0.36
93	08 / 04	08 / 04	Summer	1	2.1	106	0.11	0.24	0.03	0.047	0.41	0.51
93	08 / 27	08 / 27	Summer	1	0.7	84	0.12	0.65	0.01	0.131	1.13	0.25
93	10 / 11	10 / 11	Winter	1	3.5	83	0.44	0.55	0.27	0.054	0.12	-0.26
34		Total:		60	487.7	2,822	22.80	32.45	11.10	-----	-----	-----
Winter		Storm Average:		1.8	14.8	83	0.67	0.95	0.32	0.13	0.22	-0.13
Storms		Standardized Total Sample*:		-----	-----	-----	1.00	3.29	0.07	0.23	0.23	-0.14
		Maximum:		4	46.4	106	2.02	2.80	1.20	0.48	0.39	0.59
		Minimum:		1	1.7	31	0.12	0.21	0.03	0.02	0.11	-0.76
12		Total:		14	46.7	945	3.79	10.20	0.61	-----	-----	-----
Summer		Storm Average:		1.2	3.9	79	0.32	0.85	0.05	0.17	0.62	0.08
Storms		Standardized Total Sample*:		-----	-----	-----	1.00	5.59	0.03	0.64	0.64	0.08
		Maximum:		2	13.3	106	0.89	1.95	0.15	0.43	1.13	0.51
		Minimum:		1	0.2	52	0.11	0.24	0.01	0.05	0.30	-0.45

Table 1. Descriptive statistics for 34 winter-type and 12 summer-type storms selected for geostatistical analysis. (*Statistics for standardized total sample are unitless)

greatest variability (Figure 2). Coefficients of variation of 0.17 for winter storms and 0.51 for summer storms were indicated using linear regression, with significant correlation in both cases, and this was interpreted as a distinct proportional effect for each storm type. Sample size was not observed to be significant in determining sample variability. A comparison of the coefficient of variation with the mean storm depth for each storm indicated greater variability of the statistic for summer storms relative to winter storms, a general decrease in the variability of the statistic with an increase in mean storm depth, and also a general decrease in the value of the statistic with an increase in mean storm depth (Figure 3). Negative correlation coefficients of -.50 for winter storms and -.51 for summer storms were obtained for the coefficient of variation versus mean storm depth. Histograms of the standardized total sample (obtained by dividing the measured depth for each storm by the corresponding mean storm depth) indicated the average difference in the shape of the distribution between winter and summer storms (Figure 4). The standardized total sample coefficients of variation and the storm-average coefficients of variation for winter and summer storms were both greater than the constant values obtained using linear regression (Figure 2, 3, 4).

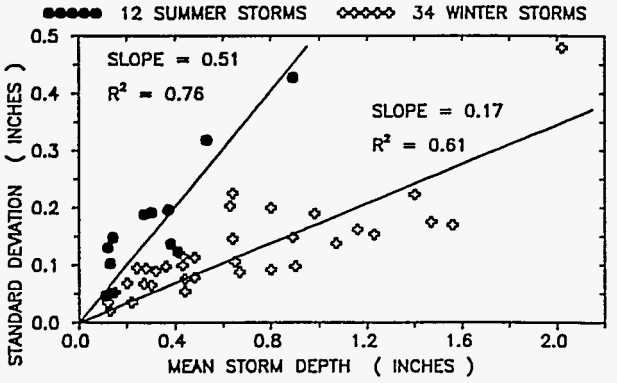

Figure 2. Standard deviation of storm precipitation depth versus mean storm depth for 34 winter-type and 12 summer-type storms recorded at Yucca Mountain.

Correlation coefficients of precipitation depth with elevation tended to be negative for winter storms and positive for summer storms (Table 1). Correlations were sometimes related to storm trajectory and the general increase in gage elevations towards the north. The predominance of negative correlations for winter storms, however, is not consistent with the known orographic influence of topography on precipitation in the southern Nevada region, which should result in a positive correlation[8,15]. A comparison of measured precipitation with gage elevation for the storm of December 7, 1992, indicated a negative quadratic trend (Figure 5). A linear correlation coefficient of -.69 was obtained for this storm (Table 1), and was interpreted as evidence of a bias in the network in terms of gage exposure; higher elevation gages tend to be more exposed to wind and thus more likely to be effected by catch deficit[5]. Catch deficit is considered a measurement error, and is usually magnified for precipitation occurring as snow due to the greater sensitivity of snow to wind effects. Measured precipitation was observed to decrease with increasing elevation above the snow line at approximately 4,200 feet for all gage types including the heated tipping bucket gages, indicating that the deficit was related to wind effects directly above the gage orifice, in addition to problems associated with measuring frozen precipitation using non-heated gages[14].

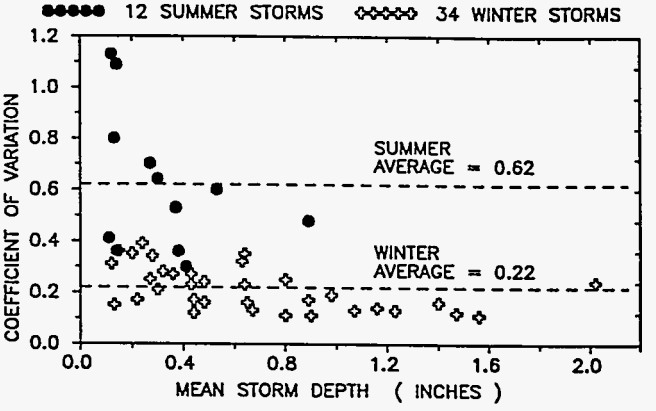

Figure 3. Coefficient of variation of storm precipitation depth versus mean storm depth.

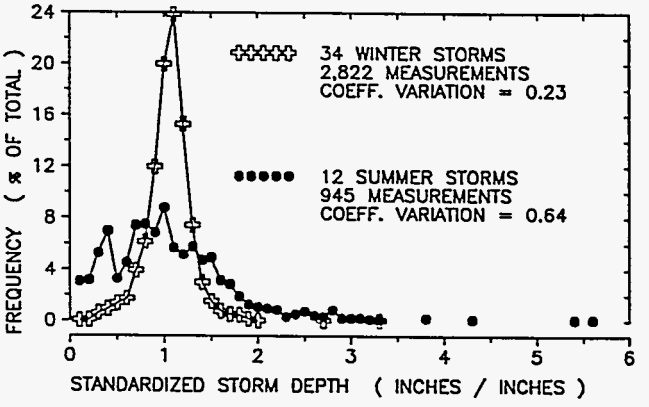

Figure 4. Histograms of the standardized total sample for 2,822 values of storm precipitation depth for winter-type storms and 945 values for summer-type storms.

Variography

A comparison of the average standardized variograms for the 34 winter storms and the 12 summer storms indicated a similarity in spatial structure (Figure 6). The variograms indicate good spatial correlation for

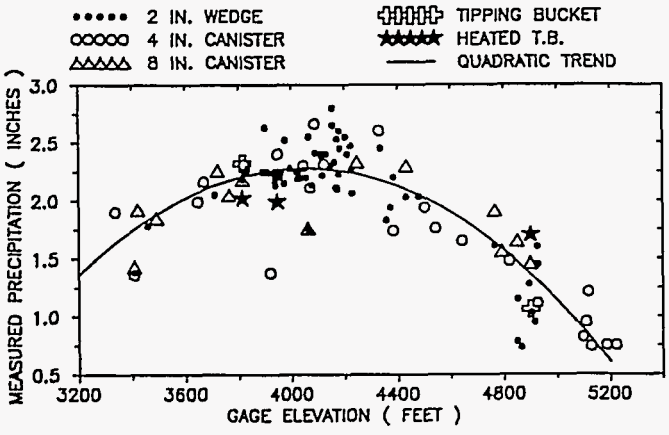

Figure 5. Measured precipitation versus gage elevation for the storm of December 7, 1992.

distances up to 20,000 feet, with small nugget structures relative to the over-all spatial variability. The variograms were also characterized by tending to values greater than unity for distances greater than 10,000 feet, indicating a trend component on the scale of the sampling domain. Trends for winter storms were attributed to the regional distribution of precipitation influenced by both meso-scale and synoptic-scale features, and also to topographic influences. For summer storms, trends were attributed to local storm cells occurring along the periphery of the network, and also to the tendency of a single, isolated cell to occur over the network per storm period. Differences between the winter and summer standardized variograms included a larger nugget structure and range of spatial correlation for the winter variogram. The winter variogram indicated more irregular behavior for distances less than 10,000 feet, and this was attributed to topographic influences on gage exposure during frontal storms.

The winter and summer storm model variograms were both defined by exponential models fitted to the standardized variograms:

$$\gamma(h) = m^2 C^2 \left[a \left(1 - EXP\left(\frac{-h}{r} \right) \right) + b \right] \qquad (5)$$

where m is the mean storm depth (inches), C is the coefficient of variation for storm depth, and h is the lag distance in feet. The model coefficients, a, r, and b, correspond to the standardized sill, range, and nugget values, respectively. For the winter model, $a = 2.4$, $r = 25{,}000$ feet, and $b = 0.13$. For the summer model, $a = 2.4$, $r = 18{,}000$ feet, and $b = 0.06$. Both models are intrinsic for distances less than approximately 30,000 feet, which is the maximum lag for which the models were considered valid. The "practical" range is 75,000 feet for the fitted winter model and 54,000 feet for the fitted summer model.

The two models were fitted to the calculated average relative sample variograms using a mean storm depth of 1.0 and the standardized total sample coefficient of variation of 0.23 for the winter model and 0.64 for the summer model (Figure 7). The summer relative variogram indicated a much greater magnitude of spatial variability relative to mean storm depth, and this was the most distinctive geostatistical difference observed between the two storm types. The relative sample variogram for summer storms indicated an apparent range of approximately 10,000 feet which was not evident in the standardized variogram, and was interpreted as a bias in the average relative spatial structure.

The winter model was fitted to the sample variogram for the winter storms of December 7, 1992 ($m = 2.02$, $C = 0.24$), and June 5, 1993 ($m = 0.65$, $C = 0.16$) (Figures 8, 9). The general fit of the average standardized model variogram to the sample variograms was considered satisfactory. Deviations from the average spatial structure were interpreted as representing differences in storm trajectory, storm intensity, wind, and precipitation occurring as snow. The standardized summer storm model also provided a satisfactory fit to the sample variograms for the storms of August 12, 1991 ($m = 0.41$, $C = 0.30$) and August 11, 1992 ($m = 0.27$, $C = 0.70$) (Figures 10, 11). In contrast to winter storms, deviations of the sample variograms from the standardized model were interpreted as differences in the position, development, and number of convective cells effecting the network. For example, the storm of August 12 resulted in measurable precipitation over the entire network, and the model provided a fairly good fit to the sample variogram. The storm of August 11, however, did not cause precipitation over the northern portion of the network, resulting in a poorer fit to the characteristic trend structure of the sample variogram.

Isohyetal Mapping of Storms

The kriging estimation method was applied using the fitted models to generate isohyetal maps for the two winter storms of December 7, 1992 and June 5, 1993, and the two summer storms of August 12, 1991 and August 11, 1992[10]. The storm of December 7 was considered representative of frontal type storms effected by topography and precipitation occurring as snow. The isohyetal map for this storm indicated a deterministic decrease in precipitation conforming to the elevation contours of Yucca Mountain (Figure 12). The storm of June 5, in contrast, did not have precipitation occurring as snow, and was not influenced by topography in terms of a catch deficit related to gage exposure. The isohyetal map for this storm indicated less variability and a general increase in precipitation towards the north (Figure 13). Although the positive correlation coefficient of 0.36 between precipitation and elevation measured for this storm is not significant, the isohyetal pattern suggested an orographic influence. The map for the August 12,

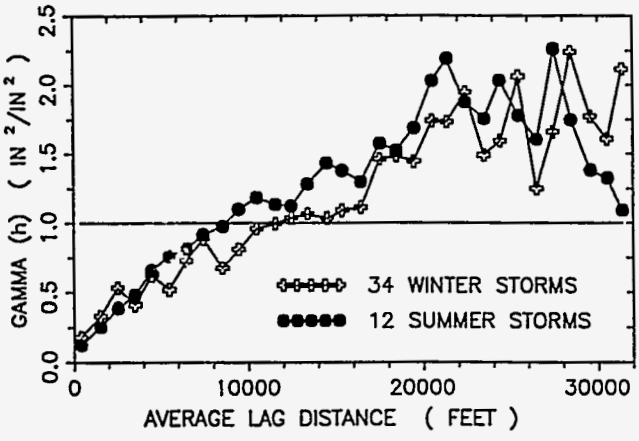

Figure 6. Comparison of winter and summer weighted-average standardized storm variograms.

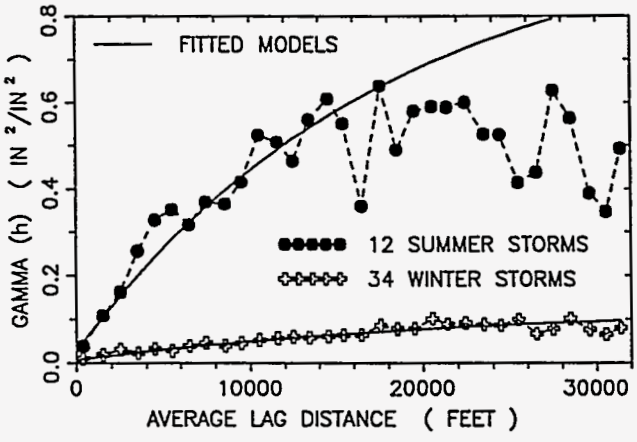

Figure 7. Comparison of winter and summer weighted-average relative storm variograms.

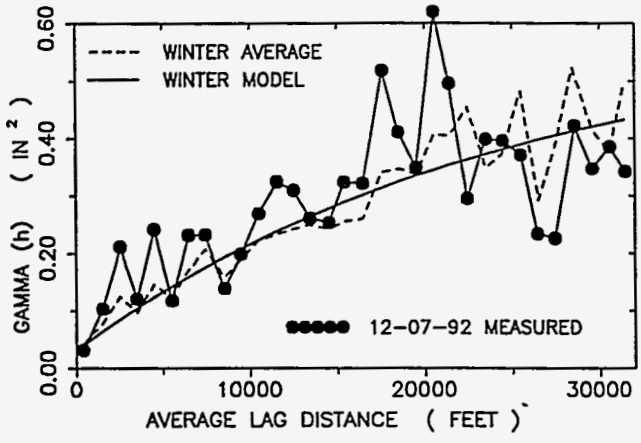

Figure 8. Sample variogram and fitted standardized model for winter storm of December 7, 1992.

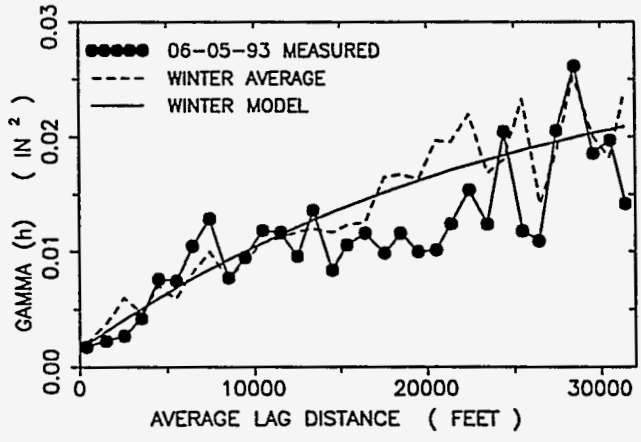

Figure 9. Sample variogram and fitted standardized model for winter storm of June 5, 1993.

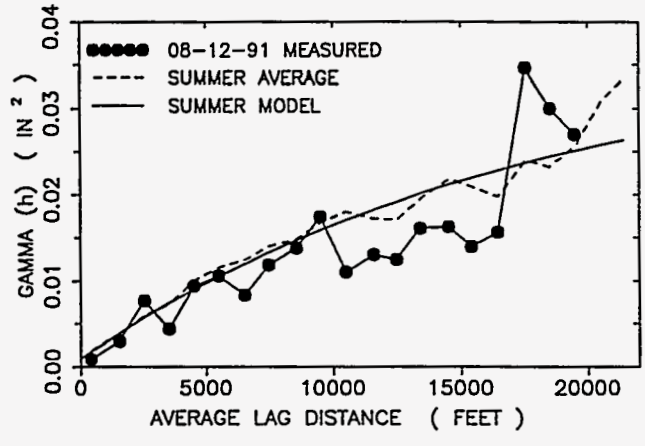

Figure 10. Sample variogram and fitted standardized model for summer storm of August 12, 1991.

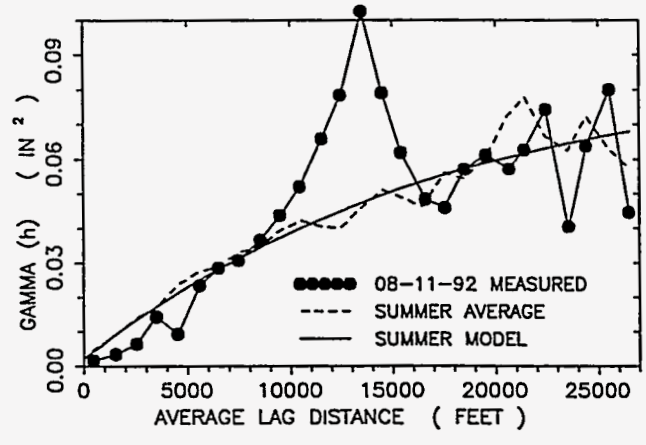

Figure 11. Sample variogram and fitted standardized model for summer storm of August 11, 1992.

1991 storm indicated a relatively irregular distribution of precipitation on the scale of the network, but the general variability was considered low for this summer-type storm (Figure 14). Three interpretations of the irregular distribution were made; 1) the convective cell was well developed and centered over the network, but precipitation within the cell was not centralized, 2) several convective cells occurred over the network, 3) the convective cell was not fully developed as it passed over the network. In contrast, the map for the storm of August 11, 1992, indicated a centralized and well defined convective cell passing over the southern portion of Yucca Mountain which was confirmed by the time-lapse video record (Figure 15). Although the spatial variability for this storm is relatively high, the isohyetal pattern is more regular and continuous, and the trend structure in the areal distribution of precipitation is distinct.

DISCUSSION

The geostatistical models presented in this study must be considered as preliminary due to; 1) an inadequate length of record which limits the number of storm periods analyzed. 2) the limited spatial coverage of the present network, especially along the periphery of the study area. 3) problems concerning measurement error (catch deficit) due to a combination of gage exposure and precipitation occurring as snow for the higher elevation gages in the network. 4) trend components in the areal distribution pattern of precipitation need to be included in the model.

The standardized models defined in this study require a-priori knowledge of the 1st and 2nd moments of precipitation depth. Mean storm depth and the coefficient of variation were used as scaling parameters instead of using the storm variance ($m^2C^2 = V$) because differences in the spatial variability between winter and summer storms were found to be characterized by the coefficient of variation. Although better fitting models might be defined for isohyetal mappings of measured precipitation depth for each recorded storm, the standardized model is a technique for predicting the spatial variability of storms likely to occur at Yucca Mountain, and was considered more applicable for the purpose of numerical storm simulation in the space-time domain. It was hypothesized that the spatial correlation model might be integrated with a stochastic model defining the temporal distribution of precipitation by using probability distribution functions for both the mean storm depth and the coefficient of variation for each storm type. It is assumed that continued monitoring of precipitation using the network of gages at Yucca Mountain will eventually provide a record sufficient for characterizing the distributions of mean storm depth and the coefficient of variation. Existing records of point precipitation having lengths of 30 to 60 years and measured at locations 12 to 100 miles from Yucca Mountain are being analyzed to characterize the temporal distribution of precipitation[5]. The temporal variability of mean storm depth might be scaled to the temporal variability of point precipitation using the central limit theorem[16]. If a characterization of the distribution of the coefficient of variation for each storm type is not possible, an average coefficient of variation for winter and summer storms would still be an improvement over assuming a single variogram model for all storm types.

SUMMARY AND CONCLUSIONS

This study presents an initial analysis and characterization of the spatial distribution of precipitation from storms measured at Yucca Mountain for a 3.8 year period from January, 1990 through October, 1993. A network of precipitation gages provided measurements of precipitation accumulated during storm periods, allowing for a geostatistical analysis of 34 winter season frontal-type storms and 12 summer season convective-type storms categorized using synoptic-scale weather patterns. Although significant variability in annual precipitation was observed, the measured storms were representative of the climate in the southern Nevada region in terms of the seasonal distribution of precipitation and synoptic-scale storm genesis.

Weighted-average standardized variograms were used to analyze differences in spatial structure between the two storm types. The standardized variograms were similar and indicated strong spatial correlation for distances less than 20,000 feet. Both variograms were characterized by an intrinsic spatial structure because the areal coverage of the network is small relative to the areal distribution of summer and winter storms. The winter variogram was characterized by more irregular behavior and increased variability for distances less than 10,000 feet because of a combination of topographic influences on gage exposure to wind and precipitation occurring as snow. Exponential models were defined for the two storm types; the winter model was defined using a standardized nugget value of 0.13 and a practical range of 75,000 feet, while the summer model was defined using a smaller standardized nugget of 0.06 and a smaller practical range of 54,000 feet. The mean storm depth and the coefficient of variation for each storm were used as scaling parameters in the standardized winter and summer models to predict the sample variograms. The average relative variogram for summer storms indicated a greater magnitude of spatial variability relative to mean storm depth as compared to the average relative variogram for winter storms, and this was found to be the most important characteristic differentiating the two storm types on the scale of the study area.

Isohyetal maps of winter storms were often characterized by topographic influences because of a decrease in measured precipitation which was attributed to an increase in gage exposure to wind with an increase in

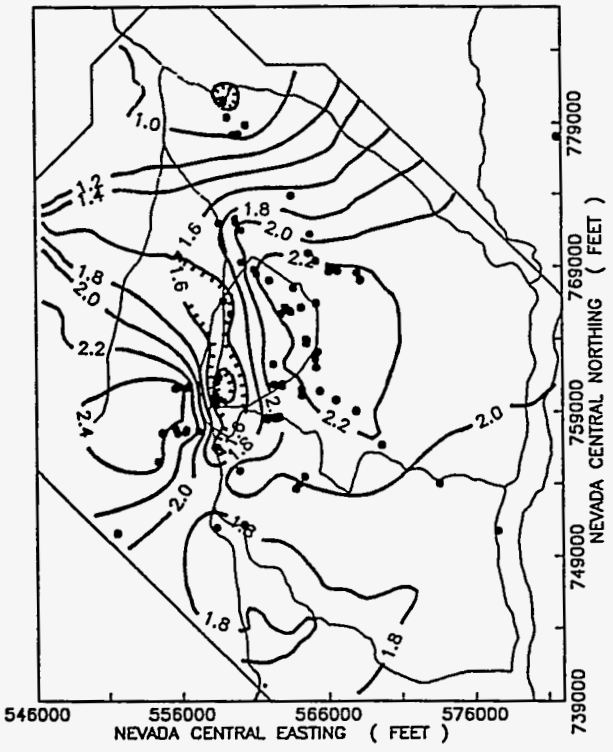

Figure 12. Kriged isohyetal map for winter storm of December 7, 1992. Isohyetal interval is 0.2 inches.

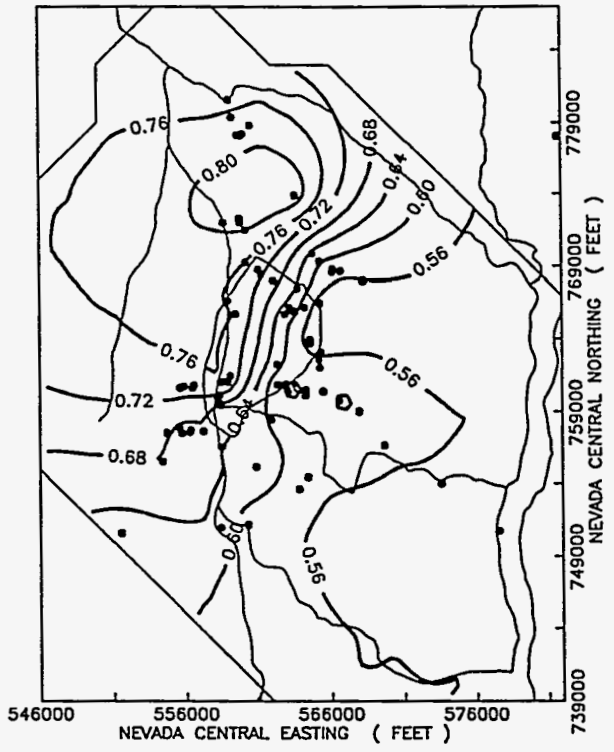

Figure 13. Kriged isohyetal map for winter storm of June 5, 1993. Isohyetal interval is 0.04 inches.

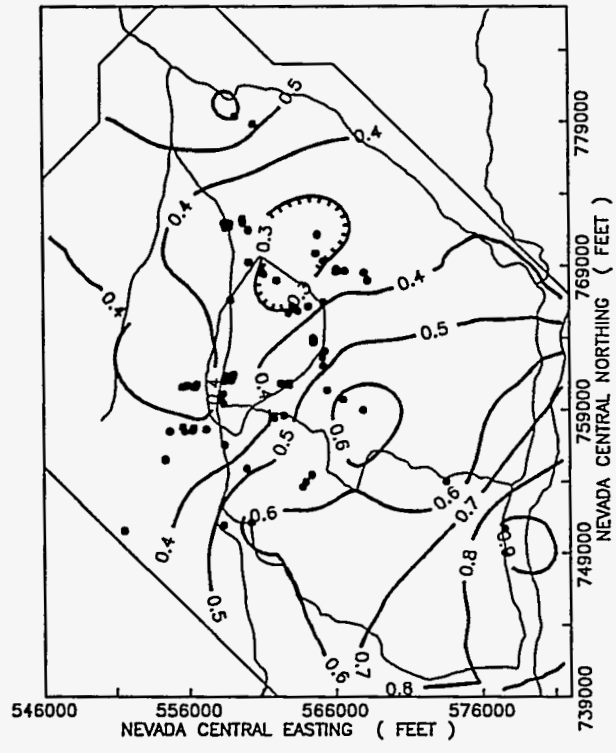

Figure 14. Kriged isohyetal map for summer storm of August 12, 1991. Isohyetal interval is 0.1 inches.

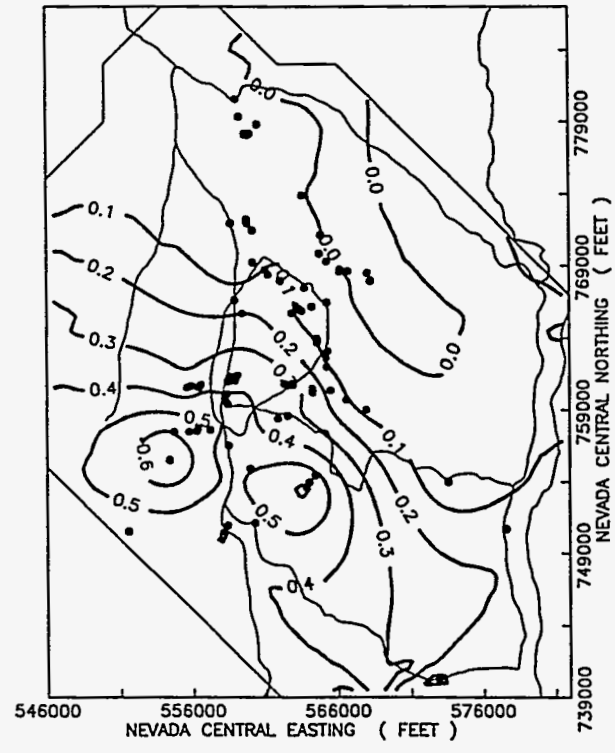

Figure 15. Kriged isohyetal map for summer storm of August 11, 1992. Isohyetal interval is 0.1 inches.

elevation, and this was considered a measurement error. The effect was not observed for all winter storms, but was most pronounced for storms with precipitation occurring as snow, and resulted in a deterministic trend component with a general increase in the spatial variability over Yucca Mountain. Isohyetal maps of summer storms indicated either well defined convective cells with a distinct trend structure, or irregular, more random patterns of precipitation depending on storm cell genesis, movement, and position relative to the network.

Although the models are considered preliminary due to the limited number of storms measured, it was concluded that the exponential models were satisfactory in predicting the spatial structure of storms if the 1st and 2nd moments of storm depth were known a-priori. Results suggest that if a probability distribution function can be defined for the two statistics, and if the trend components can be characterized and included in the model, representative simulations of storms might be possible. The current record was considered insufficient for characterizing the temporal distributions. It is hypothesized that if an adequate record can be obtained using the network of gages at Yucca Mountain, the spatial model might be integrated with a temporal model using the central limit theorem and available 30 to 60 year records of point precipitation.

REFERENCES

1. U.S. Department of Energy, *Yucca Mountain Site Characterization plan*. DOE/RW-0199, U.S. Department of Energy, Office of Civilian Radioactive Waste Management, Washington, D.C. Section 8.3.1.2.2.-1.2. (1988).

2. J.A. Hevesi, A.L. Flint, and J.D. Istok, "Precipitation Estimation in Mountainous Terrain using Multivariate Geostatistics. Part II: Isohyetal Maps", *Journal of Applied Meteorology* 31: 677-688 (1992).

3. U.S. Geological Survey, "*Characterization of the Unsaturated-Zone Infiltration, YMP-USGS-SP 8.3.-1.2.2.1., R0*", U.S. Department of Energy, Office of Civilian Radioactive Waste Management, Washington, D.C. (1990).

4. C.S. Wittwer, G.S. Bodvarsson, M.P. Chornack, A.L. Flint, L.E. Flint, B.D. Lewis, R.W. Spengler, and C.A. Rautman, "Development of a Three-Dimensional Site-Scale Model for the Unsaturated Zone at Yucca Mountain, Nevada", *Proceedings, International High Level Nuclear Waste Conference*, Las Vegas, NV., April (1992).

5. U.S. Geological Survey, "*Characterization of the Meteorology for Regional Hydrology, YMP-USGS-SP 8.3.1.2.1.1., R0*", U.S. Department of Energy, Office of Civilian Radioactive Waste Management, Washington, D.C., (1991).

6. J.A. McMahon, *Deserts, Audubon Society Nature Series*. Alfred Knopf, 368 pp. (1985).

7. R.H. French, "*A Preliminary Analysis of Precipitation in Southern Nevada*", DOE/NV/10162-10, Water Resources Center, Desert Research Institute, Las Vegas, Nevada, 39 pp. (1983).

8. R.H. French, "*Daily, Seasonal, and Annual Precipitation at the Nevada Test Site, Nevada*", U.S. Dept. of Energy, Nevada Operations Office, DE-AC08-85NV10384, Publication No. 45042, 64 pp. (1986).

9. W.D. Nichols, "Geohydrology of the Unsaturated Zone at the Burial Site for Low-Level Radioactive Waste near Beatty, Nye County, Nevada", *U.S. Geological Survey Water-Supply Paper* 2312, 57 pp. (1987).

10. A.G. Journel and C.J. Huijbregts, *Mining Geostatistics*. Academic press, 660 pp. (1978).

11. R.M. Cooper and J.D. Istok, "Geostatistics Applied to Groundwater Contamination. I: methodology", *Journal of Environmental Engineering* 114: 270-286 (1988).

12. R.M. Cooper, J.D. Istok, and A.L. Flint, "Three-Dimensional, Cross-Semivariogram Calculations for Hydrogeologic data", *Ground Water* 26: 638-646 (1988).

13. M. David, *Geostatistical Ore Reserve Estimation*. Elsevier Scientific Publishing Company, 364 pp. (1977).

14. D.S. Ambos and A.L. Flint, "Precipitation Measurements from a Network of Non-Recording Gages at Yucca Mountain, Nevada, October 1991 - April 1993", *Open-File Report*, U.S. Geological Survey, Denver, Colorado (in review) (1994).

15. J.A. Hevesi, J.D. Istok, and A.L. Flint, "Precipitation Estimation in Mountainous Terrain using Multivariate Geostatistics. Part I: Structural Analysis", *Journal of Applied Meteorology* 31: 661-676 (1992).

16. J. Devore and R. Peck, *Statistics, The Exploration and Analysis of Data*, West Publishing Company, New York, 697 pp. (1986).

HIGH LEVEL RADIOACTIVE WASTE MANAGEMENT

Proceedings of the Fifth Annual International Conference

VOLUME 4

DISCLAIMER